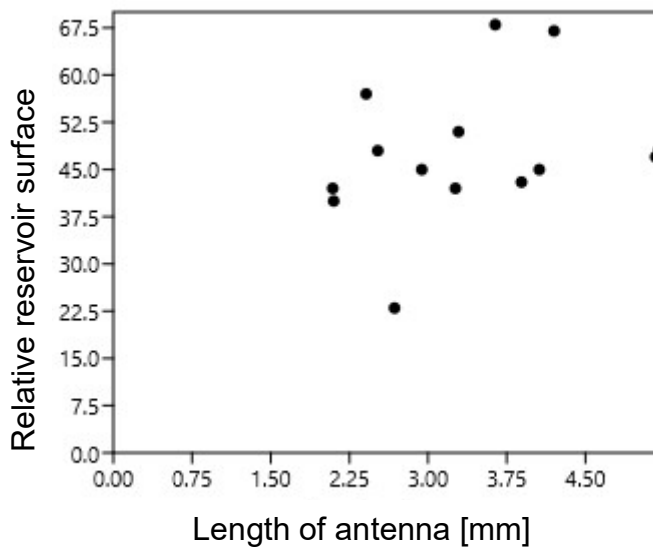
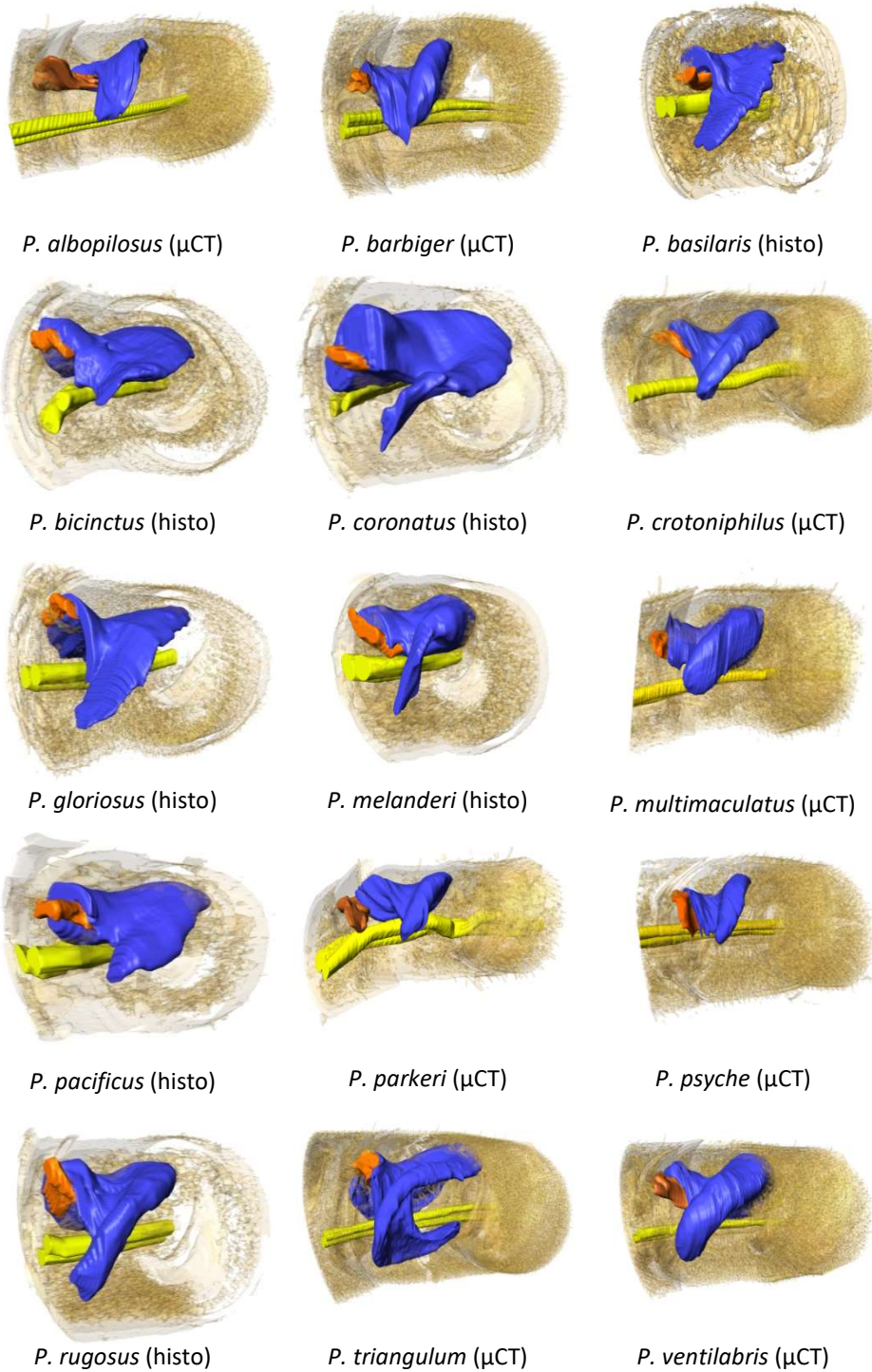


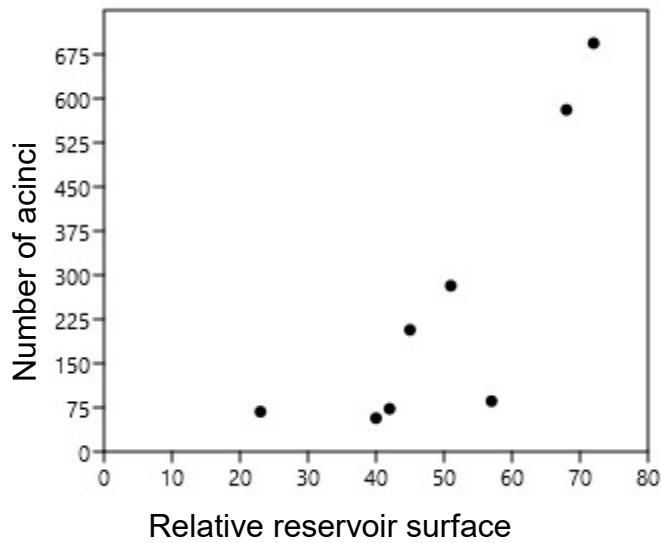
Supplementary Fig. 1 Relationship between the length of the antenna and the relative surface of the reservoir of the 6<sup>th</sup> antennomer for 15 *Philanthus* species. (Spearman correlation analysis:  $R_s = -0,08$ ,  $N = 15$ ,  $p = 0.78$ ).



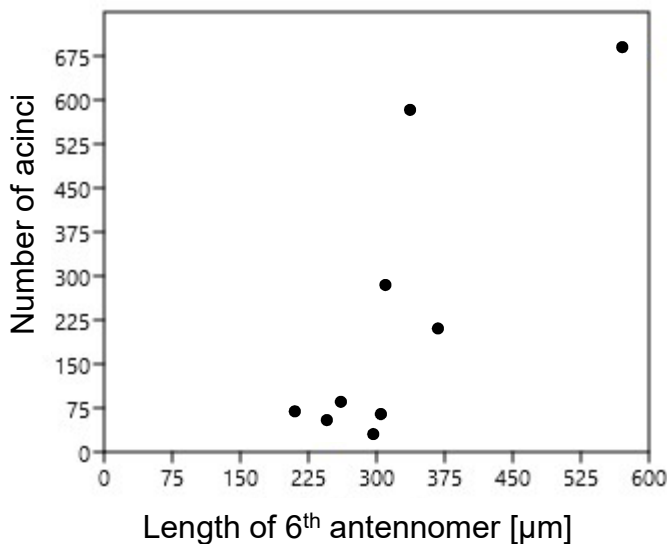
Supplementary Fig. 2 Relationship between the length of the antenna and the relative surface of the reservoir of the 6<sup>th</sup> antennomer for 15 *Philanthus* species. (Spearman correlation analysis:  $R_s = 0.28$ ,  $N = 15$ ,  $p = 0.32$ ).



Supplementary Fig. 3: 3D-models of antennal glands in antennomere A6 of females of 15 *Philanthus* species. Reconstruction was either based on histological sections (histo) or on micro-computer tomography ( $\mu$ CT). Color code: yellow, antennal nerv; orange: flap; blue: gland reservoir; the outer antennomere cuticle is displayed half transparent.



Supplementary Fig. 4 Relationship between number of acini and relative surface of the gland in the 6<sup>th</sup> antennomer for eight *Philanthus* species. The species that somewhat deviates from the trend is *P. multimaculatus* (lower right datapoint). (Spearman correlation analysis:  $R_s = 0.9$ ,  $N = 8$ ,  $p = 0.003$ ).



Supplementary Fig. 5 Relationship between the length of the 6<sup>th</sup> antennomer (μm) and the number of acini associated with the lumen of the 6<sup>th</sup> antennomer for eight *Philanthus* species. (Spearman correlation analysis:  $R_s = 0.81$ ,  $N = 8$ ,  $p = 0.018$ ).